

Self-assembled Fe nanowires using organometallic chemical vapor deposition and CaF₂ masks on stepped Si(111)

J.-L. Lin, D. Y. Petrovykh, A. Kirakosian, H. Rauscher, and F. J. Himpsel^{a)}
Physics Department, University of Wisconsin, Madison, Wisconsin 53706

P. A. Dowben
Department of Physics and Astronomy, University of Nebraska, Lincoln, Nebraska 68588

(Received 12 July 2000; accepted for publication 30 November 2000)

Linear arrays of 3 nm wide Fe stripes with 15 nm spacing are fabricated by self-assembly. They are formed by photolysis of ferrocene that is selectively adsorbed between CaF₂ stripes. An ultraviolet nitrogen laser removes the organic ligands from ferrocene. Arrays of CaF₂ stripes serve as masks, which are self-assembled on a stepped Si(111) surface. Scanning tunneling microscopy is used to investigate the surface morphology during growth. A generalization of this method to other wire materials is discussed. © 2001 American Institute of Physics. [DOI: 10.1063/1.1345830]

An important strategy for parallel fabrication of nanostructures is self-assembly. It makes it possible to manufacture macroscopic quantities of patterned materials both efficiently and economically. Here we address self-assembly of linear arrays of one-dimensional structures, or wires, on vicinal silicon surfaces. By choosing magnetic materials, such as Fe, we connect our current work with several previous studies that have been directed at the fabrication of magnetic nanostructures for patterned storage media and related applications.^{1–3} Our main focus is to develop new self-assembly methods for wires in the single-digit nanometer regime, where traditional lithography methods are not applicable.

We fabricate Fe nanowires in a three-step process: (1) prepare a silicon template with a regular array of straight steps by annealing vicinal Si(111) in a specific temperature sequence;⁴ (2) create continuous CaF₂ stripes on top of a CaF₁/Si(111) surface by growing 1–2 monolayers of CaF₂;⁵ and (3) grow Fe nanowires in the CaF₁ trenches between the CaF₂ stripes by selective adsorption of ferrocene and photolysis into Fe. We expose the patterned nanowires to ultraviolet photons from a nitrogen laser to dissociate the organic ligands from the ferrocene molecules.⁶ This photolytic process has been proven to incorporate less carbon and oxygen into the growing Fe structures than using other methods, such as pyrolysis.⁷ After the first Fe monolayer is deposited, the selective adsorption and photolysis processes continue. This is consistent with the formation of a reactive metallic Fe layer, which has a higher sticking coefficient for ferrocene than the CaF₂ mask.

Figure 1 elucidates the patterning process. It starts with vicinal Si(111) with atomically straight steps produced by resistive heating to 1250 °C followed by a sequence of annealing in an ultrahigh vacuum chamber with a base pressure 1×10^{-10} Torr: 30 s annealing at 1060 °C followed by quenching to 850 °C and a postannealing at 850 °C for 20 min.⁴ The spacing of these steps is ~15 nm, which corre-

sponds to the miscut of 1.1° used for this study combined with a step height of 0.31 nm. It can be varied by changing the substrate miscut angle. Miscuts towards $\langle \bar{1}\bar{1}2 \rangle$ generally give rise to single steps with a height of 0.31 nm. CaF₂ stripes are created by growing 1–2 monolayers of CaF₂ at a substrate temperature of ~600 °C, flashing to 830 °C (a few seconds), and postannealing at 700 °C for 4 min.⁵ Shown in the second panel of Fig. 1 is the resulting surface consisting of CaF₂ stripes on top of a CaF₁ interface layer where one fluorine atom has been desorbed to form a Ca–Si bond at the interface. Because a Ca-terminated interface is known to reverse the ABC stacking of Si(111) into CBA,^{5,8} it not only causes CaF₂ to attach to the upper edge of the steps, i.e., opposite to step flow growth, but also prevents the CaF₂ stripes on two different terraces from merging. Consequently, the CaF₁ trenches between the CaF₂ stripes remain continuous down to a width on the 1 nm scale, and continuous Fe stripes can be grown in the trenches (Fig. 2).

The top panel of Fig. 1 shows a band diagram of the CaF₂/CaF₁ masks, providing the underlying physics for selective adsorption shown in the third panel. The CaF₂ stripes retain a broad band gap of 12 eV, while the CaF₁/Si(111) interface in the trenches possesses a drastically reduced band gap of 2.4 eV.⁴ This alternating band gap with a periodicity of ~15 nm has been confirmed via chemical imaging by scanning tunneling microscopy (STM).⁹ The lowest unoccupied molecular orbital-highest occupied molecular orbital (LUMO-HOMO) band gap of ferrocene (~4.0 eV in the ground state theory, ~6 eV in the gas phase experiment, and about 4.5 eV when adsorbed on most metals surfaces) is matched better to CaF₁ than to CaF₂, facilitating the development of chemical bonds.⁷ The CaF₁/Si(111) trenches are thus chemically reactive and adsorb ferrocene molecules admitted in the gas phase, as illustrated in the third panel of Fig. 1.

Ferrocene contains one Fe atom sandwiched between two cyclopentadienyl rings (C₅H₅) and remains intact upon adsorption at substrate temperatures below ~100 °C.⁶ As the substrate is covered by ferrocene, it becomes passive unless it is exposed to ultraviolet photons. We use a commercial

^{a)}Author to whom correspondence should be addressed; electronic mail: fhimpsel@facstaff.wisc.edu

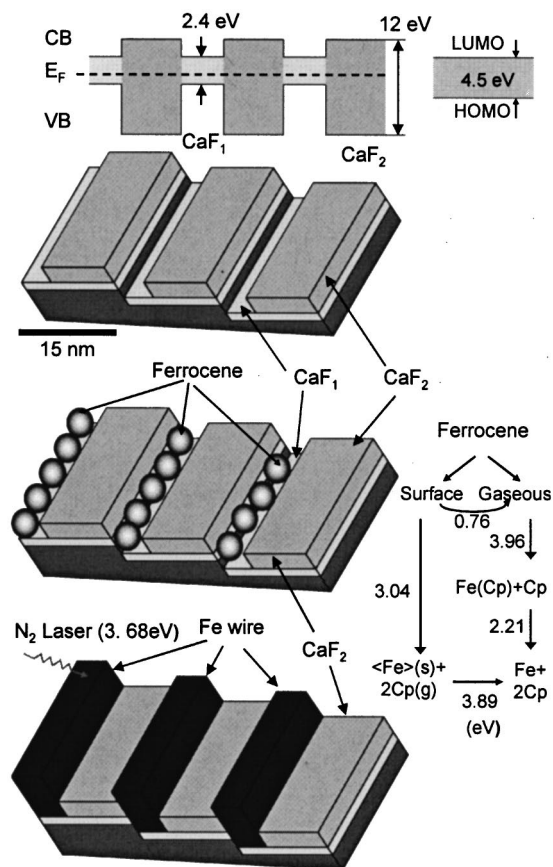


FIG. 1. Schematic of the self-assembly of Fe nanowires on stepped Si with a CaF_2 mask. (Top) Band gap modulation with a periodicity of 15 nm. CaF_1 has states that can interact with the highest occupied and lowest unoccupied orbitals of adsorbed ferrocene (HOMO and LUMO), CaF_2 does not. (Second) CaF_2 stripes on a $\text{CaF}_1/\text{Si}(111)$ surface obtained at a CaF_2 exposure between 1 and 2 monolayers. The CaF_2 stripes are attached to the upper step edges. (Third) (Left) Selective deposition of ferrocene in the CaF_1 trenches. (Right) Diagrams of energetics of ferrocene on the surface and in the gas phase. (Bottom) Deposition of Fe wires in the CaF_1 trenches after photolysis of adsorbed ferrocene. (Cp=cyclopentadienyl).

nitrogen laser with an average power of 120 mW at a repetition rate of 15 Hz. The photon energy is 3.68 eV, which is less than the binding energy between a metal atom and two C_5H_5 rings in the gas phase (6.2 eV), but sufficient to cleave the bonds between metal atoms and organic rings while the molecules are adsorbed on the surface (3.04 eV).⁷ The ferrocene pressure during growth is 1×10^{-6} Torr and the sample is resistively heated to $\sim 100^\circ\text{C}$ for 2 min every 15 min. After cycling the selective adsorption and photolysis of ferrocene processes for 90 min, Fe nanowires are deposited only onto the CaF_1 trenches, while the CaF_2 stripes are functioning as masks shaping the wires (Fig. 1 bottom).

Figure 2 shows the initial and final stages during Fe nanowire growth. The STM image at the top is taken at a bias voltage of +4 V, which allows tunneling into the conduction band of otherwise insulating CaF_2 (tunneling current 0.4 nA). The Si(111) steps are descending from left to right. Continuous CaF_2 stripes are formed on a $\text{CaF}_1/\text{Si}(111)$ interface. The coverage is about 1.9 monolayers (ML), close to the 2 ML limit above which the excess CaF_2 would cover the substrate completely.^{5,6} The stripes do not touch each other due to their topological incompatibility. The incoming ferrocene prefers to anchor at the narrow CaF_1 trenches and at

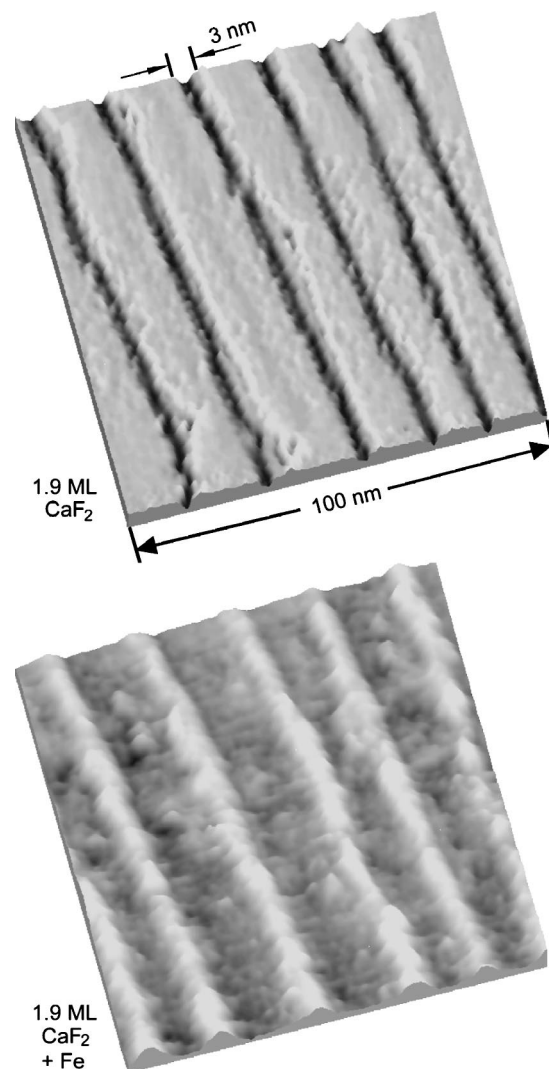


FIG. 2. STM images of the initial and final stages in the self-assembly of Fe nanowires. (Top) Wide CaF_2 stripes separated by narrow $\text{CaF}_1/\text{Si}(111)$ trenches at a coverage of 1.9 monolayers of CaF_2 . (Bottom) Linear array of Fe nanowires 3 nm wide and 0.8 nm thick, selectively deposited in the trenches by photolysis of ferrocene: $100 \times 100 \text{ nm}^2$.

the edges of the CaF_2 stripes. After photolysis of the adsorbed ferrocene molecules, the growth of Fe proceeds mainly on the CaF_1 regions, as depicted in the bottom panel of Fig. 2. The narrow trenches shown in the top panel of Fig. 2 now evolve to become ridges. These stripe-shaped protrusions on top of the CaF_1 trenches represent 3 nm wide and 0.8 nm high Fe nanowires. Guided by the continuous trenches, they grow continuously and parallel to each other. The spacing between the wires is 15 nm, in agreement with the miscut angle of 1.1° of the Si(111) template. The images in Fig. 2 were acquired at sample voltages of +4 V (top) and -1.8 V (bottom) with a tunneling current of 0.2 nA. The inversion from trenches to ridges after Fe deposition is independent of the bias voltage. A sample voltage of +4 V emphasizes tunneling into the conduction band minimum of the CaF_2 masks.^{9,10}

There are three processes leading to the selective deposition of Fe on the CaF_1 trenches. First, the deposition has to get started by selectively adsorbing ferrocene onto CaF_1 , which has orbitals that are better matched to the valence and conduction band of CaF_1 than CaF_2 (compare HOMO and

LUMO to the band edges in Fig. 1). Second, the adsorbed ferrocene layer has to be decomposed into metallic Fe by the laser. It has been suggested that ferrocene is such a stable molecule that desorption is favored over decomposition,^{11,12} which is essential to ensure that radiation-induced decomposition can indeed occur. Thermodynamic cycles of both gaseous and adsorbed ferrocene are displayed in Fig. 1.¹² Ultraviolet radiation at 337 nm (3.68 eV) provides more than sufficient energy for decomposing the ferrocene on a surface (about 3 eV) but insufficient energy for the decomposition in the gas phase (6 eV to remove both cyclopentadienyl rings and 3.96 eV to remove a single one). In fact, desorption of the fivefold cyclopentadienyl ring is observed during laser irradiation. Third, the metallic Fe layer has to remain more reactive than the CaF₂ mask in order to continue selective adsorption of ferrocene onto Fe. In general, a metallic surface is much more reactive than the insulating CaF₂ because it has a continuum of electronic states that can interact with ferrocene orbitals. Nearly metallic behavior of the Fe deposit is evident from spectroscopic STM. After photolysis we observe a stable tunneling current at small sample voltages (down to about 0.5 V), whereas the native CaF₂ surface requires a sample voltage of 4 V in order to achieve tunneling into the conduction band minimum.

Selective adsorption using CaF₂ masks on a stepped Si(111) has been observed for a variety of other molecules,¹³ and is emerging as a general method for growing one-dimensional nanostructures of transitional metals and other materials using chemical vapor deposition. The following criteria can be applied to select potential precursor molecules. The molecule should be available in the vapor phase to undergo transport to the substrate. It should have weak metal to ligand bonds and stable ligands in order to enable photolysis without leaving fragments at the surface. In the absence of radiation the precursor should not react with the surface. Various metallocenes and organometallic derivatives are likely candidates.

In Fig. 3, we show an STM image (sample voltage of +4 V) of the intermediate stage during the growth of Ni wires, i.e., selective adsorption of nickelocene at the edges and at the bottom of the CaF₁/Si(111) trenches (after 2 min postannealing at ~100 °C). A photolytic process takes place similar to that with ferrocene. The shape and width of the structures grown are determined by the morphology of the CaF₂ mask. The width can be precisely controlled by the CaF₂ coverage. The edges of the CaF₂ mask consist of atomically straight sections, following the underlying Si(111) steps.^{4,5} The spacing of the wires is dictated by the miscut angle of the vicinal Si(111). Such self-assembled CaF₂ masks on stepped Si(111) thus offer shape and size control of Fe and Ni wires on a single-digit nanometer scale.

In summary, we have described a self-assembly method that leads to arrays of Fe nanowires over macroscopic areas. Since it uses silicon as a substrate, it lends itself to integrating nanowire structures into silicon devices. This process is likely to provide a more general pathway for fabricating nanowire arrays of other materials. The deposited Fe wires

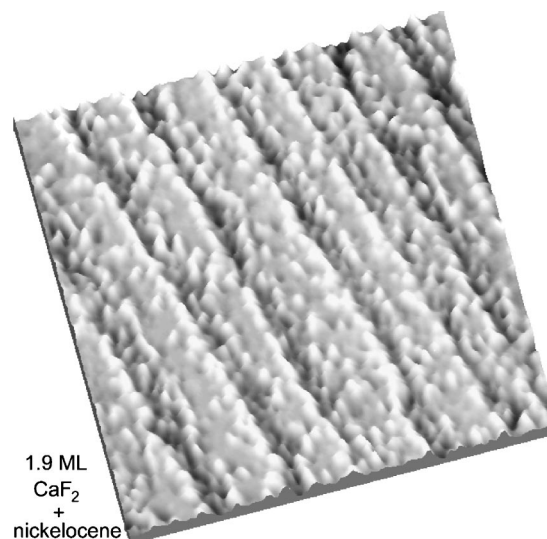


FIG. 3. Selective adsorption of nickelocene on a CaF₁/Si(111) substrate with CaF₂ stripes as masks. STM image of 100×100 nm².

are probably in the superparamagnetic regime.^{1,2} If they could be made a factor of 2–4 thicker they would become ferromagnetic and would facilitate the fabrication of fully integrated magnetoelectronic devices on a silicon substrate. Thicker wires can be expected when using a laser with a shorter wavelength that better matches the absorption of ferrocene (around 193 nm) for obtaining higher growth rates.

This work is supported by the NSF under Award Nos. DMR-0079983 and DMR-9815416. The authors thank Dr. J. Lawler and Dr. J. Curry for the technical support in using excimer lasers. They also thank J. Crain for sample characterization via near edge x-ray absorption fine structure.

¹S. Sun, C. B. Murray, D. Weller, L. Folks, and A. Moser, *Science* **287**, 1989 (2000) and references therein.

²F. J. Himpsel, J. E. Ortega, G. J. Mankey, and R. F. Willis, *Adv. Phys.* **47**, 511 (1998) and references therein.

³J. Shi, S. Gider, K. Babcock, and D. Awschalom, *Science* **271**, 937 (1996).

⁴J. Viernow, J.-L. Lin, D. Y. Petrovykh, F. M. Leibsle, F. K. Men, and F. J. Himpsel, *Appl. Phys. Lett.* **72**, 948 (1998).

⁵J. Viernow, D. Y. Petrovykh, F. K. Men, A. Kirakosian, J.-L. Lin, and F. J. Himpsel, *Appl. Phys. Lett.* **74**, 2125 (1999).

⁶J.-L. Lin, H. Rauscher, A. Kirakosian, F. J. Himpsel, and P. A. Dowben, *J. Appl. Phys.* **86**, 5492 (1999).

⁷D. Welipitiya, C. Waldfried, C. N. Borca, P. A. Dowben, N. M. Boag, H. Jiang, I. Gobulokoglu, and B. W. Robertson, *Surf. Sci.* **418**, 466 (1998); P. A. Dowben, C. Waldfried, T. Komesu, D. Welipitiya, T. McAvoy, and E. Vescovo, *Chem. Phys. Lett.* **283**, 44 (1998).

⁸M. A. Olmstead, in *Heteroepitaxial Systems*, edited by A. W. K. Liu and M. Santos (World Scientific, Singapore, 1998), Chap. 5.

⁹J. Viernow, D. Y. Petrovykh, A. Kirakosian, J.-L. Lin, F. K. Men, D. J. Seo, M. Henzler, and F. J. Himpsel, *Phys. Rev. B* **59**, 10356 (1999).

¹⁰V. P. LaBella, L. J. Schowalter, and C. A. Ventrice, Jr., *J. Vac. Sci. Technol. B* **15**, 1191 (1997).

¹¹R. Zanoni, M. N. Piancastelli, M. Marsi, and G. Margaritondo, *J. Electron Spectrosc. Relat. Phenom.* **57**, 199 (1991).

¹²D. Welipitiya, P. A. Dowben, J. Zhang, W. W. Pai, and J. F. Wendelken, *Surf. Sci.* **367**, 20 (1996).

¹³H. Rauscher, T. A. Jung, J.-L. Lin, A. Kirakosian, F. J. Himpsel, U. Rohr, and K. Müllen, *Chem. Phys. Lett.* **303**, 363 (1999).